

Quantum interference experiments with large molecules

Olaf Nairz,^{a)} Markus Arndt, and Anton Zeilinger^{b)}
Institut für Experimentalphysik, Universität Wien, Boltzmannngasse 5, A-1090 Wien, Austria

(Received 27 June 2002; accepted 30 October 2002)

Wave-particle duality is frequently the first topic students encounter in elementary quantum physics. Although this phenomenon has been demonstrated with photons, electrons, neutrons, and atoms, the dual quantum character of the famous double-slit experiment can be best explained with the largest and most classical objects, which are currently the fullerene molecules. The soccer-ball-shaped carbon cages C_{60} are large, massive, and appealing objects for which it is clear that they must behave like particles under ordinary circumstances. We present the results of a multislit diffraction experiment with such objects to demonstrate their wave nature. The experiment serves as the basis for a discussion of several quantum concepts such as coherence, randomness, complementarity, and wave-particle duality. In particular, the effect of longitudinal (spectral) coherence can be demonstrated by a direct comparison of interferograms obtained with a thermal beam and a velocity selected beam in close analogy to the usual two-slit experiments using light.

© 2003 American Association of Physics Teachers.

[DOI: 10.1119/1.1531580]

I. INTRODUCTION

At the beginning of the 20th century several important discoveries were made leading to a set of mind-boggling questions and experiments that seemed to escape any answers based on classical, pre-quantum physics. The first were the discoveries¹⁻³ that implied that optical radiation has to be composed of discrete energy packages that can be well localized in space and time. This localization was in marked contrast to the existing knowledge based on Maxwell's theory which successfully represented light as electromagnetic waves. The second and complementary breakthrough was the theoretical result by de Broglie,⁴ and the experimental demonstration by Davisson and Germer⁵ that massive particles also propagate in a wave-like manner.

Both statements were stunning at the time that they were proposed and both keep us busy thinking even today because we generally associate the notion of point-like locality with a particle while we attribute spatial extension to a wave. The observation of both phenomena in one and the same experiment leads us also to the concept of delocalization, which goes beyond the simple concept of "being extended," because single quantum objects seem to be able to simultaneously explore regions in space-time that cannot be explored by a single object in any classical way.

To illustrate the wave-particle duality we shall briefly recall the double-slit experiment as sketched in Fig. 1 because it is both one of the simplest and most general quantum experiments used in introductory quantum physics and is the prototype for our studies with molecules.

Let us first discuss an experiment that is usually performed in a ripple tank. If we excite surface waves in water and let them propagate through a small hole in a barrier (Fig. 1, left), we would observe a circular wavelet emerge behind the barrier in agreement with Huygens' principle. If we now open a second hole in the barrier, we could create regions where the water remains completely still (Fig. 1, center). This phenomenon is simply explained by the fact that the surface waves superpose on each other and the wave minima can be filled by wave maxima at well-determined places. We call this phenomenon interference. It can only be easily ob-

served if the disturbances in the two slits are synchronized with each other, which means that they have a well-defined and constant phase relation, and may therefore be regarded as being coherent with respect to each other.

For water the picture appears intuitive because the wave is composed of many particles, each interacting with its neighbors. But the experiment turns into the mind-boggler mentioned above if we repeat it with an ensemble of isolated objects—photons or even massive particles—which we send through the double-slit one by one.

We shall present experimental results with, at present, the most massive particles that exhibit wave properties. The results confirm that under appropriate circumstances we still obtain interference patterns, the shape of which can be predicted with certainty. However, it is important to note that in such investigations a single particle always gives a single click at one detector position only, and we have no means of calculating the position of this event in advance because, as far as we can tell, it is governed by chance.

Therefore, the double-slit experiment with single particles leads us to the following questions: How can a single particle, which we observe both in the source and in the detector as being well-localized and much smaller than a single opening in the barrier, acquire information about the state (open/closed) of a very remote opening, if it were considered to pass only one through the openings? Why can't we track the particle position without destroying its wave nature? How can we understand the emergence of a well-defined interference pattern in contrast to the random hitting point of the single object if none of the particles can interact with the rest of the ensemble in any way that we know?⁶

We thus find many fundamental quantum concepts in the context of double-slit interferometry. First, we find the complementarity between our knowledge about the particle's position and the visibility of the interferogram. If we open one slit only, the particle must pass this opening and the interference pattern must disappear. Perfect interference contrast can be obtained only if we open the second slit and if we exclude all possibilities of detecting, even in principle, the path the object has taken. The wave-particle duality states that the description of one and the same physical ob-

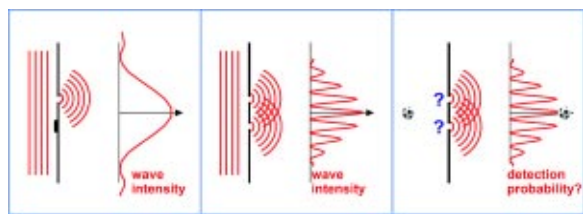


Fig. 1. The double-slit experiment is the prototype experiment demonstrating the wave–particle duality in quantum mechanics. (a) A wave impinging on a wall with one sufficiently small slit will spread out behind this obstacle. An explanation based on Huygen’s principle tells us that each point in the wave front can be imagined as being a source of a spherical wavelet. The fields of many such sources interfere on the screen and form the single slit pattern. (b) If we open a second slit, which sees the same wave as the first one, the field amplitude at a sufficiently long distance from the slits drops to zero at specific points: we observe destructive interference due to the overlap of wave troughs and hills. (c) Which pattern can we expect if we replace the continuous source by one that emits quanta, that is, discrete packages of energy and/or mass that are well localized in space and time in the source? Can a single particle as massive as a buckyball acquire information of two spatially separate locations?

ject suggests the local particle picture in the source and on the screen, but a wave model for the unobserved propagation of the object. Mathematically we describe the state of the particle during the propagation as a superposition of states, in particular of position states, that are classically mutually exclusive. A classical object will either take one or the other path. A quantum object cannot be said to do that. The intrinsic information content of the quantum system itself is insufficient to allow such a description—even in principle.⁷ We also find the duality between objective randomness and determinism. The pattern on the screen is well determined for the ensemble, but the detection point of a single object is completely unpredictable in all experiments.

All of these “quantum mysteries” imply that in an experiment the possibility of having a position is often the only objective reality in contrast to the property of having a well-defined position.

These reasons are why Richard Feynman emphasized that the double-slit experiment is at the heart of quantum mechanics:⁸ “In reality, it contains the only mystery, the basic peculiarities of all of quantum mechanics.” We might suggest that another central issue of quantum physics, namely entanglement, is missing in this example. However, it turns out to be an essential ingredient if we consider how we could diffuse which-path information to the environment—a phenomenon leading to loss of coherence between the neighboring paths in the double-slit experiment.

The fact that the wave nature of matter is a cornerstone of quantum mechanics, but that this very feature completely escapes perception in our everyday life, is one of the remarkable properties of this theory. The smallness of Planck’s constant and therefore of the de Broglie wavelength of a macroscopic object is certainly largely responsible for the nonobservability of quantum effects in the classical world. However, it is interesting to ask whether there are limits to quantum physics and how far we can push the experimental techniques to visualize quantum effects in the mesoscopic world for objects of increasing size, mass, and complexity.

We shall therefore briefly review the experimental efforts in this field throughout the last century. Soon after Louis de Broglie’s proposed wave hypothesis for material particles, matter wave phenomena were experimentally verified for

electrons,⁵ atoms and dimers,⁹ and neutrons.^{10,11} Young’s double-slit experiment with matter waves was then done by Jönsson for electrons,¹² by Zeilinger and collaborators for neutrons,¹³ by Carnal and Mlynek for atoms,¹⁴ and by Schöllkopf and Toennies for small molecules and noble gas clusters.^{15,16}

Further advances in matter wave physics with atoms were made possible by sophisticated techniques exploiting the interaction between atoms and light. Already in 1975 ideas were put forward for slowing and cooling of atoms using light scattering.^{17,18} The rapid progress of this field was recognized by the fact that the most important developments in this field were recently awarded the Nobel prize for laser cooling^{19–21} in 1997 and for the experimental realization of Bose–Einstein condensates with dilute atomic vapor^{22,23} in 2001. In Bose–Einstein condensates all atoms have extremely long de Broglie wavelengths and are coherent over macroscopic distances up to a millimeter. However, similar to light quanta in a laser beam, the atoms in a Bose–Einstein condensate are kept sufficiently apart to keep their interaction weak. Therefore, in spite of the large coherence length, the interfering object is still of small mass and complexity. Even experiments demonstrating interference between two Bose–Einstein condensates²⁴ can be viewed as a double-slit experiment with many individual atoms, as witnessed also by the fact that to explain the fringe spacing the de Broglie wavelength corresponding to the individual atom rather than a wavelength using the total mass of the condensate is used.

Different questions and new experimental challenges arise if we study particles in the almost opposite parameter regime where the interaction among the particles is much stronger. Covalently bound atoms form a new entity, a molecule or cluster, and the de Broglie wavelength of this system is defined by the total mass of all the atoms and by the center-of-mass velocity of the bound system. In the following we shall focus on these complex objects.

The very first demonstration of molecule interference dates back to the days of Estermann and Stern⁹ in 1930, who demonstrated experimentally diffraction of H_2 at a LiF crystal surface. Further experiments with diatomic molecules had to await progress and interest in atom optics. A Ramsey–Bordé interferometer was already realized for the iodine dimer in 1994²⁵ and was recently used²⁶ for K_2 . Similarly, a Mach–Zehnder interferometer was demonstrated²⁷ for Na_2 . The near-field analog to the Mach–Zehnder interferometer, a Talbot–Lau interferometer, was recently applied to experiments with Li_2 .²⁸ Diffraction at nanofabricated gratings also turned out to be the most effective way to prove the existence of the weakly bound helium dimer¹⁶ and to measure its binding energy.²⁹

Based on these historical achievements we ask how far we might be able to extend such quantum experiments and for what kind of objects we might still be able to show the wave–particle duality. Recently, a new set of experiments exceeding the mass and complexity of the previously used objects by about an order of magnitude has been developed in our laboratory. These experiments with the fullerene molecule C_{60} will be described in Sec. II.

II. THE C_{60} EXPERIMENT

The cage-like carbon molecules earned their names “fullerenes” and “buckminsterfullerenes” because of their close resemblance to geodesic structures that were first discussed by Leonardo da Vinci³⁰ and implemented in buildings



Fig. 2. The fullerene molecule C_{60} , consisting of 60 carbon atoms arranged in a truncated icosahedral shape, is the smallest known natural soccer ball.

in the United States by the architect Buckminster Fuller.³¹ This new modification of pure carbon was discovered in 1985 by Kroto *et al.*³² and shown to be particularly stable and abundant when exactly 60 carbon atoms are arranged in one molecule to form the smallest natural soccer ball we know, the buckyball, as shown in Fig. 2.

Fullerenes are appealing candidates because a successful quantum experiment with them would be regarded as an important step toward the realm of our macroscopic world: Many of the known physical properties of buckyballs are more closely related to a chunk of hot solid material than to the cold atoms that have so far been used in matter wave interference. The existence of collective many-particle states like plasmons and excitons, the rich variety of vibrational and rotational modes as well as the concept of an internal molecular temperature are only some of the clear indicators of the multiparticle composition of the fullerenes. And we might wonder whether this internal complexity could spoil the quantum wave behavior of the center of mass motion.

To answer this question, we have set up a new experiment as shown in Fig. 3. It resembles very much the standard Young's double-slit experiment. Like its historical counterpart, our setup also consists of four main parts: the source, the collimation, the diffraction grating, and the detector.

A. The source

To bring the buckyballs into the gas phase, fullerene powder is sublimated in a ceramic oven at a temperature of about 900 K. The vapor pressure is then sufficient to eject molecules, in a statistical sequence, one by one through a small slit in the oven. The molecules have a most probable velocity v_{mp} of about 200 m/s and a nearly thermal velocity spread of $\Delta v/v_{mp} \approx 60\%$. Here Δv is the full width of the distribution at half height.

To calculate the expected diffraction angles, we first need to know the de Broglie wavelength which is uniquely determined by the momentum of the molecule

$$\lambda = \frac{h}{mv}, \quad (1)$$

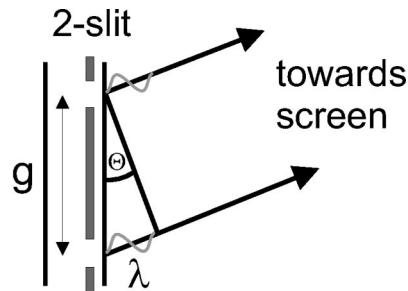
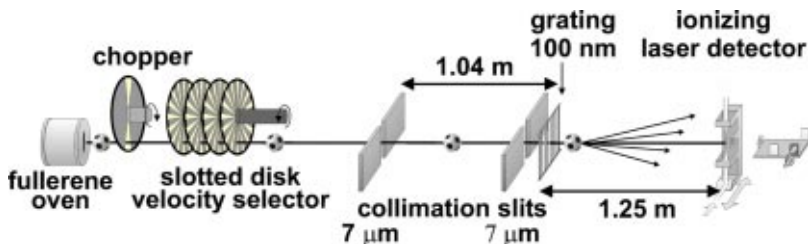


Fig. 4. Textbook approach to double-slit diffraction. First-order interference maxima of a monochromatic wave are caused by constructive interference of the wavelets that emerge from two neighboring slits. The corresponding path length difference between the two paths is equal to the de Broglie wavelength. Higher order interference will be spoiled by the limited longitudinal coherence in a thermal source. Velocity selection in our experiments increases the longitudinal coherence length by more than a factor of 3 and therefore permits the observation of higher order interference fringes.

where h is Planck's constant. Accordingly, for a C_{60} fullerene with a mass of $m = 1.2 \times 10^{-24}$ kg and a velocity of $v = 200$ m/s, we find a wavelength of $\lambda = 2.8$ pm.³³

B. The diffractive element

Because the de Broglie wavelength is about five orders of magnitude smaller than any realistic free-standing mechanical structure, we expect the characteristic size of the interference phenomena to be small. A sophisticated machinery is therefore necessary to actually show them. As the diffracting element we used a free-standing silicon nitride grating with a nominal grating constant of $d = 100$ nm, slit openings of $s = 55 \pm 5$ nm and thickness of only 200 nm along the beam trajectory. These gratings are at the cutting edge of current technology and only a few specialists worldwide can actually make them.³⁴

We can now calculate the deflection angle to the first diffraction order in the small angle approximation as the ratio of the wavelength and the grating constant,

$$\theta = \frac{\lambda}{d} = \frac{2.8 \times 10^{-12} \text{ m}}{10^{-7} \text{ m}} = 28 \text{ } \mu\text{rad}. \quad (2)$$

In elementary textbooks Eq. (2) is usually derived using Fig. 4 and noting that the first constructive interference occurs when the difference between two neighboring paths is equal to one de Broglie wavelength. Because our detector is placed at 1.2 m downstream from the grating, the separation between the interference peaks at the detector amounts then to only $L \times \theta = 1.2 \text{ m} \times 28 \text{ } \mu\text{rad} = 34 \text{ } \mu\text{m}$.

Fig. 3. Setup of the diffraction experiment. Fullerene molecules are sublimated in the oven at 900 K. The spectral coherence can be improved using a mechanical velocity selector. Two collimating slits improve the spatial coherence and limit the angular spread of the beam to smaller than the expected diffraction angle. A SiN grating with a 100 nm period and 50 nm openings is used to diffract the incident molecular waves. The molecular far-field distribution is observed using a scanning laser-ionization detector.

C. The detector

The small spacing between the interference orders requires a high spatial resolution of the molecule detector. For the fullerenes we have implemented a novel detector that surpasses most other schemes in detection efficiency, spatial resolution, and simplicity.

A continuous-wave green laser beam (argon ion laser, all lines) with a full power of 25 W is focused to the beam width of only $4\ \mu\text{m}$. As shown in Fig. 3, the laser beam is orthogonal to the molecular beam. All molecules that pass the laser beam at or very close to the focus are heated to an internal temperature in excess of 3000 K and ionize. The positive fullerene ions are then accelerated toward an electrode at 10 kV where they induce the emission of electrons. The electrons in turn are again multiplied and the charge pulses are subsequently counted. The overall molecule detection efficiency is about 10% and thus about two orders of magnitude higher than for example, electron beam bombardment ionization as used in many mass spectrometers. We find that among all gases in our vacuum chamber, the laser detector is only sensitive to fullerenes, due to the particular level scheme and high stability against fragmentation. Because of the tight focusing of the laser beam, the effective width of our detector³⁵ amounts to only $\sim 8\ \mu\text{m}$, which is sufficient to resolve the individual diffraction orders. To record a diffraction pattern, we scan the laser across the molecular beam in steps of $2\ \mu\text{m}$. The interferograms shown below represent molecule counts as a function of the transverse laser position.

D. Coherence considerations

Let us now turn to the coherence properties of our molecular beam. In general, coherence means that there is a fixed and well-defined phase relation in space and time between two or more wave fronts.

The spatial (transverse) coherence of our source is almost negligible right after the oven. Inside the source, the coherence width is actually only of the order of the thermal de Broglie wavelength. As is true in general for extended sources with uncorrelated emitters, the visibility is then reduced by the fact that the many partial interferometers—each starting at one point in the source and forming two trajectories through the double-slit toward a point in the detector—acquire different phase differences along their path to a given spot on the screen.

After the oven, we therefore need to enlarge the spatial coherence width by about five orders of magnitude in order to illuminate at least two neighboring slits coherently. Luckily, the spatial coherence is essentially determined by the geometry of the experiment and grows linearly to a good approximation with increasing distance from the source and with decreasing size of the first collimation slit. This general rule for the influence of collimating elements on transverse coherence is commonly known as the van Cittert–Zernike theorem.³⁶ The spatial coherence function can be derived from diffraction curves which are determined by the apertures along the molecular beam. The limiting element in our case is the first collimation slit.

Obviously the gain in coherence has to be paid for by a dramatic drop in the count rate because the signal decreases quadratically with the distance from the source and linearly with the size of the slit. Although the first collimating slit alone already provides coherence, we still have to introduce a second collimating slit—in our case also $7\ \mu\text{m}$ wide and

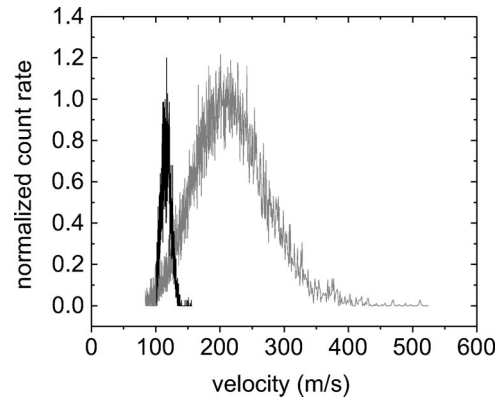


Fig. 5. Velocity distribution of the C_{60} molecules for a thermal and a velocity selected beam. The thermal beam (gray curve) is centered around $\bar{v} = 200\ \text{m/s}$ and has a width of $\Delta v/v \sim 0.6$, while the selected beam (black curve) is centered around $\bar{v} = 117\ \text{m/s}$ with a width of $\Delta v/v \sim 0.17$. We therefore expect the velocity selected interference pattern to be expanded by 70% on the screen and to show at least three times ($\approx 0.6/0.17$) as many interference orders as the unselected pattern.

about 1 m downstream from the first slit. The reason for this is the requirement that the collimated beam width needs to be significantly smaller than the separation between the diffraction orders behind the grating in order to clearly resolve the diffraction peaks.

The spectral coherence of the source also enters because molecules with different velocities and therefore different wavelengths follow different diffraction angles. And because the detector records the sum of the correspondingly stretched or compressed diffraction pictures, the interference pattern would be washed out. And in contrast to the spatial contribution, there is no gain in longitudinal (spectral) coherence during free flight. This is due to the fact that different velocity classes will evolve differently. In a pulsed beam experiment we would therefore observe a chirped packet, that is, a wave packet with short wavelengths in the pulse lead and long wavelengths in its tail. And even though the packet would spread out in the course of its evolution, the coherence would not grow due to the internal rearrangement.

Although even in pulsed experiments the spectral coherence does not improve during propagation because of the internal restructuring of the wave packet, the picture of a wave packet is problematic for the description of a continuous source. It is unfounded because the wave packet picture implies a well-defined internal phase structure. More specifically, a wave packet is characterized by a well-defined phase relation between different Fourier components of the beam. Yet such a relation can only be imposed by a suitable preparation. In our case that would imply a well-defined time at which the wave packet starts. This is not provided in our experiment, and the beam can be regarded only as a statistical, and therefore incoherent, mixture of the various momenta. Nevertheless, the beam can operationally be characterized by a coherence length, which is the length that measures the falloff of the interference visibility when the difference between two interfering paths increases. The longitudinal coherence length is given by³⁷ $L_c \approx \lambda^2/\Delta\lambda = \lambda v/\Delta v$.

For our thermal beam with $\Delta v/v \sim 0.6$ we find $L_c \sim 1.7\lambda$, which is just enough to guarantee the existence of the first-order interference fringes. We shall later discuss the

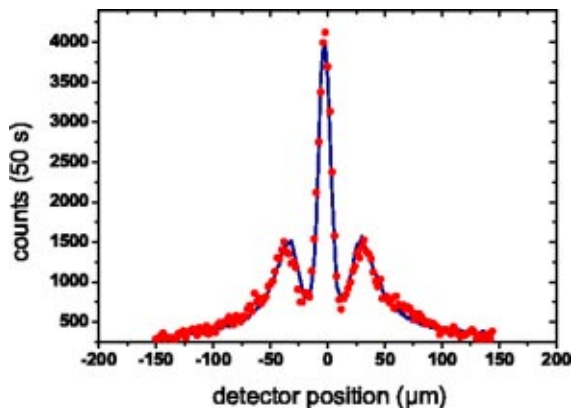


Fig. 6. Far-field diffraction of C_{60} using a thermal beam of $\bar{v} = 200$ m/s with a velocity spread of $\Delta v/v \sim 60\%$. The absence of higher order interference fringes is due to the poor spectral coherence.

improvement of the spectral purity using a velocity filter (see Figs. 3 and 5), thereby also improving the wavelength distribution.

Figure 6 shows a typical fullerene diffraction pattern with a thermal beam. We can clearly discern the first interference orders on both sides of the central peak. But the limited coherence is reflected by the fact that we cannot see any second or higher order peaks in the interferogram of Fig. 6.

To see more fringes we have to increase the coherence length and therefore decrease the velocity spread. For this purpose we have employed a mechanical velocity selector, as shown after the oven in Fig. 3. It consists of four slotted disks that rotate around a common axis. The first disk chops the fullerene beam and only those molecules are transmitted that traverse the distance from one disk to the next in the same time that the disks rotate from one open slot to the next. Although two disks would suffice for this purpose, the additional disks decrease the velocity spread even further and help eliminate velocity sidebands. By varying the rotation frequency of the selector, the desired velocity class of the transmitted molecules can be adjusted. To measure the time of flight distribution we chopped the fullerene beam with the

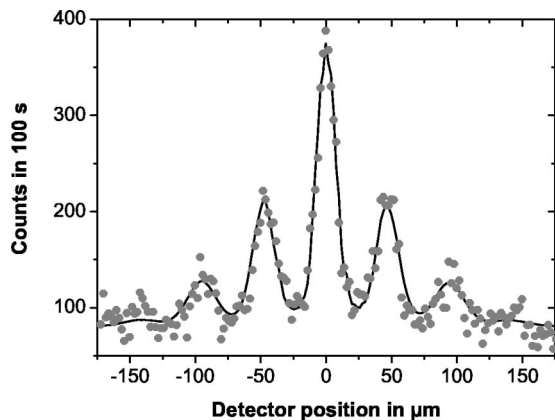


Fig. 7. Far-field diffraction of C_{60} using the slotted disk velocity selector. The mean velocity was $\bar{v} = 117$ m/s, and the width was $\Delta v/v \sim 17\%$. Full circles represent the experimental data. The full line is a numerical model based on Kirchhoff–Fresnel diffraction theory. The van der Waals interaction between the molecule and the grating wall is taken into account in form of a reduced slit width. Grating defects (holes) additionally contribute to the zeroth order.

chopper right behind the source (see Fig. 3). The selection is of course accompanied by a significant loss in count rate, but we can still retain about 7% of the unselected molecules.

In Fig. 5 both the thermal and the selected velocity distributions are shown. In contrast to the width of the thermal spectrum, amounting to $\Delta v/v = 60\%$, we are able to reduce this number to only 17% with the selector. The increase in longitudinal coherence by a factor of more than 3 allows for the observation of diffraction peaks up to at least the second and possibly the third order, as can be seen in Fig. 7.

It should also be pointed out that by using the velocity selector, we can now choose a slow mean velocity centered about 120 m/s, which corresponds to a de Broglie wavelength of 4.6 pm. It is obvious that this increase in wavelength results in a wider separation of the diffraction peaks, which can be seen by comparing Figs. 6 and 7.

In principle, the diffraction patterns can be understood quantitatively within the Fraunhofer approximation of Kirchhoff's diffraction theory as it can be found in any optics textbook.³⁸ However, Fraunhofer's diffraction theory in the context of optics misses an important point that becomes evident in our experiments with matter waves and material gratings: the attractive interaction between molecule and wall results in an additional phase of the molecular wave function after the passage of the molecule through the slits.³⁹ Although the details of the calculations are somewhat involved,⁴⁰ it suffices here to say that the qualitative effect of this attractive force can be understood as a narrowing of the real slit width toward an *effective* slit width. For our fullerene molecules the reduction can be as big as 20 nm for the unselected molecular beam and almost 30 nm for the velocity selected beam. The stronger effect on slower molecules can be understood by the longer and therefore more influential interaction between the molecules and the wall. However, a complete description would need to take into account the correct shape of the complex (imaginary and real) transmission function, which implies the position-dependent modulation of both the molecular amplitude and phase.

The full lines in Figs. 6 and 7 are fits of our data to this modified Kirchhoff–Fresnel theory. To obtain such a good fit we also have to take into account an enhanced contribution in the zeroth order which we attribute to mechanical defects (holes) of the grating which are significantly larger than the grating period.

III. CONCLUDING REMARKS

A. Single particle interferometry

It is important to note that the interference pattern is built up from single, separate particles. There is no interference *between* two or more particles during their evolution in the apparatus. Single particle interference is evidenced in our case by two independent arguments.

The first argument is based on the spatial separation between the molecules. The molecular flux at an average speed of 200 m/s is $\sim 3 \times 10^9$ cm⁻² s⁻¹ at the plane of the detector. This flux corresponds to an average molecular density of 1.7×10^{11} m⁻³ or an average molecular distance of 200 μm. This is three orders of magnitude wider than any realistic range of molecular (van der Waals) forces, which are typically confined to several 100 nm.

The second argument is based on the fact that interference occurs only between indistinguishable states. However, all molecules may be regarded as being in different states. There

are 174 different vibrational modes and the rotational modes can be populated at different energies. The chance of having two subsequent molecules in exactly the same state of all internal modes is vanishingly small. Therefore, interference in our experiments really is a single particle phenomenon!

B. Coherence and which-path information

We might believe that coherence experiments could be spoiled by transitions between the many thermally excited states. Obviously, this is not the case, as has been shown by our experiments. But why is this so? No matter what we do, we can only observe one of these qualities in its ideal form at any given time. If we tried to locate the particle during its passage through one of the two slits, say by blocking one of the openings, the interference pattern would disappear. This rule still holds if we do not block the slit, but manage to obtain which-path information for example via photons scattered or emitted by the molecules. Sufficiently complex molecules, in contrast to the electrons, neutrons, and atoms used so far, may actually emit radiation^{41,42} without any external excitation, because they have stored enough thermal energy when leaving the oven. According to Bohr's rule, the interference pattern must then disappear if the molecules emit a photon with a sufficiently short wavelength which enables the experimenter to measure the location of the emitting molecule with sufficient precision. According to Abbé's theory of the microscope, the photon should have a wavelength shorter than twice the distance between the two slits.

What actually saves the experiment is the weakness of the interaction. The wavelength of the most probably emitted photons is about a factor of 100 larger than the separation between two neighboring slits. And the number of light quanta that actually leak into the environment is still sufficiently small—of the order of one, up to potentially a few photons—and cannot disturb the interference measurably. Therefore, even if the fullerene molecule emits a few photons on its path from the source to the detector, these photons cannot yet be used to determine the path taken by the molecule. In other words, the photon state and the molecule state are not (or only very slightly) entangled because the two possible photon emission states from either path largely overlap. In a sense we may say that the fullerene has no “memory” along which path the emission occurred.

C. Conclusion

Quantum phenomena become increasingly important and the limit to which we may be able to confirm all quantum principles experimentally is still an open question. The discussion of our fullerene experiments lets us demonstrate the basic wave–particle duality for the most massive, most complex, and most “classical” single object so far. Many of the concepts that we teach our students can be illustrated simply. For instance, the notion of coherence length has a rather intuitive meaning when we compare the spectral width of the source and the number of observed interference fringes.

ACKNOWLEDGMENTS

This work has been supported by the European TMR network, Contract No. ERBFM-RXCT960002, by the Austrian Science Foundation (FWF), within Project Nos. SFB F1505 and START Y177 (MA). ON acknowledges a scholarship by the Austrian Academy of Sciences.

^{a)}Also at: Université de Genève, GAP-Optique, Rue de l'École-de-Médecine 20, CH-1211 Genève 4.

^{b)}Electronic mail: zeilinger-office@exp.univie.ac.at

¹M. Planck, “Zur Theorie des Gesetzes der Energieverteilung im Normalenspektrum,” Verh. Dtsch. Phys. Ges. **2**, 237 (1900); English translation: “On the theory of the energy distribution law of the normal spectrum,” in *The Old Quantum Theory*, edited by D. ter Haar (Pergamon, New York, 1967), p. 82.

²P. Lenard, “Über die lichtelektrische Wirkung,” Ann. Phys. (Leipzig) **8**, 149–198 (1902).

³A. Einstein, “Über einen die Erzeugung und Verwandlung des Lichtes betreffenden heuristischen Gesichtspunkt,” Ann. Phys. (Leipzig) **17**, 132–148 (1905); English translation: A. Arons and M. Peppard, “Concerning an heuristic point of view toward the emission and transformation of light,” Am. J. Phys. **33**, 367–374 (1965).

⁴L. de Broglie, “Waves and quanta,” Nature (London) **112**, 540–540 (1923).

⁵C. Davisson and L. Germer, “The scattering of electrons by a single crystal of nickel,” Nature (London) **119**, 558–560 (1927).

⁶A student, having been taught some elementary statistical physics, would be tempted to answer the second one by analogy with the Galton board. Also there, the trajectory of the single particle appears to be undetermined and still the count rate in each channel would be in agreement with the deterministic laws of classical statistics. But we should note, first of all, that the apparent randomness in this example is only due to the ill-defined initial conditions when we release the ball. Second, if we were to perform such a Galton experiment with two different starting positions, the probability distributions of these experiments would simply add up and interference would never be observed.

⁷C. Brukner and A. Zeilinger, “Young's experiment and the finiteness of information,” Philos. Trans. R. Soc. London, Ser. A **360**, 1061–1069 (2002).

⁸R. P. Feynman and A. R. Hibbs, *Quantum Mechanics and Path Integrals* (McGraw-Hill, New York, 1965).

⁹I. Estermann and O. Stern, “Beugung von Molekularstrahlen,” Z. Phys. **61**, 95–125 (1930).

¹⁰H. v. Halban Jnr. and P. Preiswerk, “Preuve Expérimentale de la Diffraction Des Neutrons,” C. R. Acad. Sci. Paris **203**, 73–75 (1936).

¹¹R. Gähler and A. Zeilinger, “Wave-optical experiments with very cold neutrons,” Am. J. Phys. **59**, 316–324 (1991).

¹²C. Jönsson, “Electron diffraction at multiple slits,” Am. J. Phys. **42**, 4–11 (1974).

¹³A. Zeilinger, R. Gähler, C. G. Shull, W. Treimer, and W. Mampe, “Single- and double-slit diffraction of neutrons,” Rev. Mod. Phys. **60**, 1067–1073 (1988).

¹⁴O. Carnal and J. Mlynek, “Young's double-slit experiment with atoms: A simple atom interferometer,” Phys. Rev. Lett. **66**, 2689–2692 (1991).

¹⁵W. Schöllkopf and J. P. Toennies, “Nondestructive mass selection of small van der Waals clusters,” Science **266**, 1345–1348 (1994).

¹⁶W. Schöllkopf and J. Toennies, “The nondestructive detection of the Helium dimer and trimer,” J. Chem. Phys. **104**, 1155–1158 (1996).

¹⁷T. W. Hänsch and A. L. Schawlow, “Cooling of gases by laser radiation,” Opt. Commun. **13**, 68–69 (1975).

¹⁸D. Wineland and H. Dehmelt, “Proposed $10^{14}\Delta\nu < \nu$ laser fluorescence spectroscopy on Ti^+ mono-ion oscillator III (side band cooling),” Bull. Am. Phys. Soc. **20**, 637–637 (1975).

¹⁹S. Chu, “The manipulation of neutral particles,” Rev. Mod. Phys. **70**, 685–706 (1998).

²⁰C. N. Cohen-Tannoudji, “Manipulating atoms with photons,” Rev. Mod. Phys. **70**, 707–719 (1998).

²¹W. D. Phillips, “Laser cooling and trapping of neutral atoms,” Rev. Mod. Phys. **70**, 721–741 (1998).

²²M. H. Anderson, J. R. Ensher, M. R. Matthews, C. E. Wieman, and E. A. Cornell, “Observation of Bose–Einstein condensation in a dilute atomic vapor,” Science **269**, 198–201 (1995).

²³K. B. Davis, M.-O. Mewes, M. R. Andrews, N. J. van Druten, D. S. Durfee, D. M. Kurn, and W. Ketterle, “Bose–Einstein condensation in a gas of Sodium atoms,” Phys. Rev. Lett. **75**, 3969–3973 (1995).

²⁴M. R. Andrews, C. Townsend, H. Miesner, D. Durfee, D. Kurn, and W. Ketterle, “Observation of interference between two Bose condensates,” Science **275**, 637–641 (1997).

²⁵C. Bordé, N. Courtier, F. D. Burck, A. Goncharov, and M. Gorlicki, “Molecular interferometry experiments,” Phys. Lett. A **188**, 187–197 (1994).

²⁶C. Lisdat, M. Frank, H. Knockel, M.-L. Almazor, and E. Tiemann, “Re-

- alization of a Ramsey–Bordé matter wave interferometer on the K_2 molecule,” *Eur. Phys. J. D* **12**, 235–240 (2000).
- ²⁷M. S. Chapman, C. R. Ekstrom, T. D. Hammond, R. A. Rubenstein, J. Schmiedmayer, S. Wehinger, and D. E. Pritchard, “Optics and interferometry with Na_2 molecules,” *Phys. Rev. Lett.* **74**, 4783–4786 (1995).
- ²⁸See comment by J. Clauser in *Atom Interferometry*, edited by P. R. Berman (Academic, New York, 1997), p. 143.
- ²⁹R. E. Grisenti, W. Schöllkopf, J. P. Toennies, G. C. Hegerfeldt, T. Köhler, and M. Stoll, “Determination of the bond length and binding energy of the Helium dimer by diffraction from a transmission grating,” *Phys. Rev. Lett.* **85**, 2284–2287 (2000).
- ³⁰L. Saffaro, “Cosmoids, fullerenes and continuous polygons,” in *Proceedings of the First Italian Workshop on Fullerenes: Status and Perspectives*, edited by C. Taliani, G. Ruani, and R. Zamboni (World Scientific, Singapore, 1992), Vol. 2, p. 55.
- ³¹R. W. Marks, *The Dymaxion World of Buckminster Fuller* (Southern Illinois U.P., Carbondale, 1960).
- ³²H. Kroto, J. Heath, S. O’Brian, R. Curl, and R. Smalley, “C₆₀: Buckminsterfullerene,” *Nature (London)* **318**, 162–166 (1985).
- ³³It is interesting to compare the de Broglie wavelength of the fullerene with its actual size: The buckyball has a diameter of about 1 nm, which is 350 times larger than its de Broglie wavelength. Our interference experiments clearly show that the concept of the de Broglie wavelength is not merely academic for objects with dimensions much larger than their wavelengths but can actually be demonstrated.
- ³⁴Our gratings were provided by Professor Henry Smith and Dr. Tim Savas of MIT.
- ³⁵M. Arndt, O. Nairz, J. Voss-Andreae, C. Keller, G. van der Zouw, and A. Zeilinger, “Wave-particle duality of C₆₀ molecules,” *Nature (London)* **401**, 680–682 (1999); O. Nairz, M. Arndt, and A. Zeilinger, “Experimental challenges in fullerene interferometry,” *J. Mod. Opt.* **47**, 2811–2821 (2000).
- ³⁶For the original work see P. V. Cittert, “Die wahrscheinliche Schwingungsverteilung in einer von einer Lichtquelle direkt oder mittels einer Linse beleuchteten Ebene,” *Physica (Amsterdam)* **1**, 201–210 (1934), and F. Zernike, “The concept of degree of coherence and its application to optical problems,” *ibid.* **5**, 785–795 (1938). A textbook with a detailed account of the theorem is M. Born and E. Wolf, *Principles of Optics* (Pergamon, New York, 1993).
- ³⁷L. Bergmann and C. Schaefer, *Optics: Of Waves and Particles* (de Gruyter, New York, 1999).
- ³⁸E. Hecht, *Optics* (Addison-Wesley, Reading, MA, 2002), 4th ed.
- ³⁹This effect has also been described in the context of He diffraction in R. E. Grisenti, W. Schöllkopf, J. P. Toennies, G. C. Hegerfeldt, and T. Köhler, “Determination of atom-surface van der Waals potentials from transmission-grating diffraction intensities,” *Phys. Rev. Lett.* **83**, 1755–1758 (1999).
- ⁴⁰The van der Waals interaction scales like r^{-3} with the distance r between molecule and grating walls. For C₆₀ the scaling even starts to change into a r^{-4} behavior at distances beyond 20 nm, due to the finite (retarded) signaling time between the molecule and its mirror image; see also H. B. G. Casimir and D. Polder, “The influence of retardation on the London-van der Waals forces,” *Phys. Rev.* **73**, 360–372 (1948).
- ⁴¹R. Mitzner and E. E. B. Campbell, “Optical emission studies of laser desorbed C₆₀,” *J. Chem. Phys.* **103**, 2445–2453 (1995).
- ⁴²K. Hansen and E. Campbell, “Thermal radiation from small particles,” *Phys. Rev. E* **58**, 5477–5482 (1998).

Erratum: “Quantum interference experiments with large molecules” [Am. J. Phys. 71 (4), 319–325 (2003)]

Olaf Nairz,^{a)} Markus Arndt, and Anton Zeilinger^{b)}
Universität Wien, Institut für Experimentalphysik, Boltzmanngasse 5, A-1090 Wien, Austria

[DOI: 10.1119/1.1603277]

In Fig. 3 the correct distance between grating and detector was $L = 1.20 \pm 0.01$ m as also stated in the text.

In the caption to Fig. 7 the mean velocity in the experiment of Fig. 7 was experimentally determined to be $\bar{v} = 136 \pm 3$ m/s instead of $\bar{v} = 117$ m/s as stated in the caption for Fig. 7. Note, that the mean velocity in Fig. 7 was selected

to be higher than that of Fig. 5 in order to utilize a more intense part of the thermal velocity distribution.

^{a)}Now at St. Johanns-Spital, Landesklinik für Radiotherapie und Radio-Onkologie, Müllner Hauptstrasse 48, 5020 Salzburg.

^{b)}Electronic mail: zeilinger-office@exp.univie.ac.at

Erratum: “One century later: Remarks on the Barnett experiment” [Am. J. Phys. 71 (6), 558–561 (2003)]

Alexander L. Kholmetskii^{a)}
Department of Physics, Belarus State University, 4, F. Skorina Avenue, 220080 Minsk, Belarus

[DOI: 10.1119/1.1604388]

The derivation in Eqs. (4)–(8) follows closely that found in “Vacuum Electrodynamics on a Merry-Go-Round” by John Ise and Jack Uretsky [Am. J. Phys. 26, 431–435 (1958)]. I thank Jack Uretsky for bringing this reference to my attention.

^{a)}Electronic mail: kholm@bsu.by